International Journal of Electrical, Electronic and Communication Sciences
ISSN: 2517-9438
Vol:9, No:3, 2015

Nanostructured Pt/MnO_2 Catalysts and Their Performance for Oxygen Reduction Reaction in Air Cathode Microbial Fuel Cell

Maksudur Rahman Khan, Kar Min Chan, Huei Ruey Ong, Chin Kui Cheng, Wasikur Rahman

***Abstract*—**Microbial fuel cells (MFCs) represent a promising technology for simultaneous bioelectricity generation and wastewater treatment. Catalysts are significant portions of the cost of microbial fuel cell cathodes. Many materials have been tested as aqueous cathodes, but air-cathodes are needed to avoid energy demands for water aeration. The sluggish oxygen reduction reaction (ORR) rate at air cathode necessitates efficient electrocatalyst such as carbon supported platinum catalyst (Pt/C) which is very costly. Manganese oxide (MnO_2) was a representative metal oxide which has been studied as a promising alternative electrocatalyst for ORR and has been tested in air-cathode MFCs. However the single MnO_2 has poor electric conductivity and low stability. In the present work, the MnO_2 catalyst has been modified by doping Pt nanoparticle. The goal of the work was to improve the performance of the MFC with minimum Pt loading. MnO_2 and Pt nanoparticles were prepared by hydrothermal and sol gel methods, respectively. Wet impregnation method was used to synthesize Pt/MnO_2 catalyst. The catalysts were further used as cathode catalysts in air-cathode cubic MFCs, in which anaerobic sludge was inoculated as biocatalysts and palm oil mill effluent (POME) was used as the substrate in the anode chamber. The as-prepared Pt/MnO_2 was characterized comprehensively through field emission scanning electron microscope (FESEM), X-Ray diffraction (XRD), X-ray photoelectron spectroscopy (XPS), and cyclic voltammetry (CV) where its surface morphology, crystallinity, oxidation state and electrochemical activity were examined, respectively. XPS revealed Mn (IV) oxidation state and Pt (0) nanoparticle metal, indicating the presence of MnO_2 and Pt. Morphology of Pt/MnO_2 observed from FESEM shows that the doping of Pt did not cause change in needle-like shape of MnO_2 which provides large contacting surface area. The electrochemical active area of the Pt/MnO_2 catalysts has been increased from 276 to 617 m^2/g with the increase in Pt loading from 0.2 to 0.8 wt%. The CV results in O_2 saturated neutral Na_2SO_4 solution showed that MnO_2 and Pt/MnO_2 catalysts could catalyze ORR with different catalytic activities. MFC with Pt/MnO_2 (0.4 wt% Pt) as air cathode catalyst generates a maximum power density of 165 mW/m^3, which is higher than that of MFC with MnO_2 catalyst (95 mW/m^3). The open circuit voltage (OCV) of the MFC operated with MnO_2 cathode gradually decreased during 14 days of operation, whereas the MFC with Pt/MnO_2 cathode remained almost constant throughout the operation suggesting the higher stability of the Pt/MnO_2 catalyst. Therefore, Pt/MnO_2 with 0.4 wt% Pt successfully demonstrated as an efficient and low cost electrocatalyst for ORR in air cathode MFC with higher electrochemical activity, stability and hence enhanced performance.

***Keywords*—**Microbial fuel cell, oxygen reduction reaction, Pt/MnO_2, palm oil mill effluent, polarization curve.

Md. Maksudur Rahman Khan is with the Faculty of Chemical and Natural Resources Engineering, Universiti Malaysia Pahang, 26300 Gambang, Pahang, Malaysia (corresponding author to provide phone: +0060169596643; fax: +006095492889; e-mail: mrkhancep@yahoo.com).

Kar Min Chan, Huei Ruey Ong, Chin Kui Cheng, and Md. Wasikur Rahman are with the Faculty of Chemical and Natural Resources Engineering, Universiti Malaysia Pahang, 26300 Gambang, Pahang, Malaysia (e-mail: karminchan@live.com.my, roi_rui86@hotmail.com, chinkui@ump.edu.my, wasikurjstu@gmail.com).

I. Introduction

THE major concerns of present time are energy crisis and wastewater treatment issue. Following the rapid advancement in civilization, energy demand of mammoth capacity is constantly on the rise. Looking at the fact that approximately 80% of world energy are derived from depleting fossil fuels such as natural gas, coal and petroleum which are on the brink of exhaustion, the effort in searching for sustainable new renewable energy source is indispensable. Moreover, the discharge of wastewater is increasing in line with the rapid development and substantial amount of energy is required to treat the wastewater generated. This can be exemplified in United States where roughly 5% of the total electricity generated is used for wastewater treatment plant solely [1]. The high energy requirement has been the constant concern which critically needs promising alternative to resolve. Microbial fuel cells (MFCs) represent a novel and promising technology for the generation of alternative power and wastewater treatment [2]. The main advantage of MFC technology is direct electricity generation from low grade substrates. The nature of substrate used as source of energy in the anode of MFC, greatly affects the electricity production [3]. The domestic and industrial wastewaters instead of pure substrates are been extensively studied in recent years [4]-[7].

In Malaysia, the abundance of oil palm industries has contributed to the generation of massive amount of palm oil mill effluent (POME). Around 3 tonnes of POME is generated with every tonne of crude palm oil produced. The existing POME treatment methods are inefficient as they are highly energy intensive, aerobic treatment, in particular [8], [9]. In order to make it energy efficient POME has recently been investigated as a potential substrate in MFC [10]. In their study, a two-chamber MFC was used and it was found that the low strength (low Chemical Oxygen Demand) POME is preferable in order to achieve high efficiency in the MFC. In the two-chamber MFC, the catholyte is usually $KMnO_4$ and it requires extra space to operate. Air cathode MFCs are a variation of MFC where the cathode compartment is exposed to the air. In the air-cathode MFC, due to the reduction of molecular oxygen in cathode, it is the best choice for both

chemical fuel cells and for MFCs, because the reduction product is clean, non-polluting H_2O. Oxygen reduction reaction (ORR) requires electrocatalyst for its sluggish rate. Hence, the type of electrocatalyst is vital in influencing the performance of MFCs. Platinum supported on carbon, Pt/C is the common efficient catalyst used in ORR but its application is limited due to high cost [11], [12]. Alternatively, efforts in the search for low cost catalysts are on the way. Non-noble catalyst such as manganese dioxide (MnO_2) is among metal oxides which has been well studied and giving promising result in MFC performance [13], [14]. However, stability issue was found in MnO_2. Doping of novel metals, such as Pt or Au can improve the performance and the stability of the catalysts. Doping of novel metals, such as Pt or Au nanoparticles (NPs) on supports has many advantages, such as increasing the number of surface atoms and thus active sites, bringing synergistic effects between NP and support, and lowering the cost of catalysts [15]. The control of the novel metal loading is a critical issue for electrocatalyst synthesis.

The goal of the present work is to synthesize Pt/MnO_2 nanostructured catalysts with minimum loading of platinum to generate higher power and achieve higher COD removal efficiency in the air-cathode MFC. The catalytic performance of Pt/MnO_2 catalysts with varied Pt loadings were evaluated for ORR.

II. Materials and Methods

A. Chemicals and Raw Materials

Potassium permanganate ($KMnO_4$, 99%), sulphuric acid (H_2SO_4, 96%), methanol (CH_3OH, 30%), trisodium citrate dihydrate ($C_6H_9Na_3O_9$, 99%), hexachloroplatinic acid hexahydrate ($H_2Pt_4Cl_6.H_2SO_4$, 99%), isopropanol (C_3H_8O, 96%), Nafion solution (5 wt%) and digestion solution were purchased from Sigma Aldrich and used without further purification. Polyacrylonitrile carbon felt (PACF) and Nafion 117 membrane were procured from Du Pont (USA). Palm oil mill effluent (POME) and anaerobic sludge were collected from FELDA palm oil plant located at Panching, Pahang.

B. Manganese Dioxide Preparation

Manganese dioxide (MnO_2) was synthesized by the reduction of potassium permanganate ($KMnO_4$) in aqueous sulphuric acid solution (H_2SO_4) by hydrothermal treatment as described by [16]. Specifically, 4 g of $KMnO_4$ powder was added into 200 mL of 2.5M H_2SO_4 aqueous solution and was heated at 80 °C for 30 minutes under stirring. The precipitates were produced and the solution colour was changed. The reaction course was monitored by the colour change from dark purple to dark brown. The solution was then cooled down to room temperature naturally. Subsequently, the precipitate (MnO_2) was filtered by using filter paper and washed thoroughly with distilled water to remove all the possible remaining ions, then dried for 48 h in a vacuum oven (Haier, 2450 MHz, 700 W) at 80°C.

C. Platinum sols Preparation

Platinum (Pt) sols containing Pt nanoparticles with an average size of 2–3 nm were prepared by the method described elsewhere [17]. Briefly, a mixture of 5 mL of 0.1M hexachloroplatinic acid (H_2PtCl_6) aqueous solution and 0.17 g of trisodium citrate dihydrate ($C_6H_9Na_3O_9$) powder was added to 45 mL of methanol solution under reflux and stirring at 80°C. The reaction was stopped by quenching to room temperature immediately after the solution turned into dark brown.

D. Pt/MnO_2 Preparation and Characterization

Pt/MnO_2 nanostructured catalyst with a Pt loading of 0.2, 0.4 and 0.8 wt%, respectively were prepared by wet impregnation method. In brief, 20 mg of MnO_2 was mixed with 3, 5, and 10 mL of Pt sols each, respectively and ultrasonicated at 65°C until the solvents were evaporated, which thereafter, was washed with deionised (DI) water and filtered. The mixture was then dried for 24 h in vacuum oven (Haier, 2450 MHz, 700 W) at 65°C.

The catalysts were characterized through field emission scanning electron microscope (FESEM), X-ray diffraction (XRD), and X-ray photoelectron spectroscopy (XPS) (XPSPEAK version 4.1) to examine its morphological surface, crystal structure and chemical states, respectively.

E. Electrode Preparation

The prepared catalyst (10 mg) was dispersed evenly on polyacrylonitrile carbon felt (PACF) with a thickness of 2 mm. The area of catalyst dispersion was 7cm^2. The suspension of catalyst powder for deposition was made by mixing with 0.15 mL of 5 wt% Nafion solution and 0.15 mL of isopropanol (C_3H_8O) and subjected to ultra-sonification for 20 min. The nafion 117 membrane with a dimension of 5 cm x 5 cm was boiled in 0.1M H_2SO_4 solution for 30 min, followed by boiling in deionized water for 1 h. Pretreated membranes were kept in deionized water overnight at room temperature before use. The membrane-electrode-assembly (MEA) was prepared by hot pressing catalyst/PACF with the pretreated nafion 117 membrane for 2 min at both sides. The press temperature was set at 100°C and the press pressure was 1 bar. The steps were repeated in the fabrication of electrodes with different loadings of Pt. A sample without Pt was also prepared and investigated as a control.

F. MFC Construction and Operation

The air cathode single chamber MFC was built with a cubic plexi glass which has a dimension of 5 cm x 5 cm (Shanghai, Sunny Scientific, China) and a total working volume of 20 mL. Carbon brush was directly used as anode electrode. The MEA was placed at the front opening side of the cubic chamber by facing the membrane side to the anode substrate and the PACF side was faced to the air. The whole MFC setup was tighten up with screws. Titanium wire of 5 cm was inserted through the MEA. Electric circuit consisting of resistor was connected from the anode chamber of MFC to the cathode chamber. The raw palm oil mill effluent (POME) diluted with deionized water with ratio of 1:49 was used as anode substrate of air cathode MFC. Anaerobic sludge was collected from currently running anaerobic digester of palm

oil industry (FELDA) at Panching, Pahang to be used as inoculum in the anode chamber of air cathode MFC. The ratio of anaerobic sludge to the diluted POME is 1:25. The anode chamber was flushed with N_2 for 1 h and tightly closed. For comparing the performance of MFCs, four air-cathode single chamber MFC reactors with MnO_2, and Pt/MnO_2 with three different loadings were set up for the study. All experiments were conducted at room temperature. For wastewater characterization, required amount of sample was withdrawn from anode chamber after two weeks of MFC operation. The COD was determined using digestive solution (0 – 1500 mg/L range; Hach, USA) and measured using a COD reactor (HACH DRB 200, USA).

G. Electrochemical Characterization and Analysis

To determine the ORR activity of the catalysts, cyclic voltammetry (CV) was performed using an electrochemical workstation (AUTOLAB 2273, PAR, USA) with a three-electrode configuration consisting of an Ag/AgCl serving as the reference electrode, a working electrode of catalyst coated carbon papers, and a platinum mesh counter electrode placed in 20 mL 0.1M Na_2SO_4 solution aerated by oxygen for 1.5 h. To determine the electrochemical active area, N_2 saturated 0.1M H_2SO_4 electrolyte solution was used. The scan rate was fixed at 0.03 mV/s. The Pt active surface-area was calculated by integrating the charge of the hydrogen desorption region in the cyclic voltammogram, with double-layer charge correction and a conversion factor of 210 Ccm^{-2} Pt.

Polarization measurements were performed to determine the power generation of MFC at different external resistance from 50 Ω to 500,000 Ω using an external resistor (Fluke 289 true RMS digital multimeters). Polarization curves were obtained from the corresponding voltage data which were taken after the readings stabilized for at least 5 min. Current density and power density were normalized to the geometric volume of the MFC (20 cm^3). Power (P, mW), power densities (P_v, W/m^3) and current density (I_v, A/m^3) were calculated based on:

$$P = VI \tag{1}$$

$$P_v = \frac{V^2}{R_v} \tag{2}$$

$$I_v = \frac{V}{R_v} \tag{3}$$

where, V is the cell voltage (V), R is the external resistor (Ω), and V is the volume of the MFC (m^3). The open circuit voltages (OCVs) of MFCs were measured using a potentiostat.

The COD was determined using digestive solution (0 – 1500 mg/L range; Hach, USA) and measured using a COD reactor (HACH DRB 200, USA).

III. Results and Discussion

A. Field Emission Scanning Electron Microscope

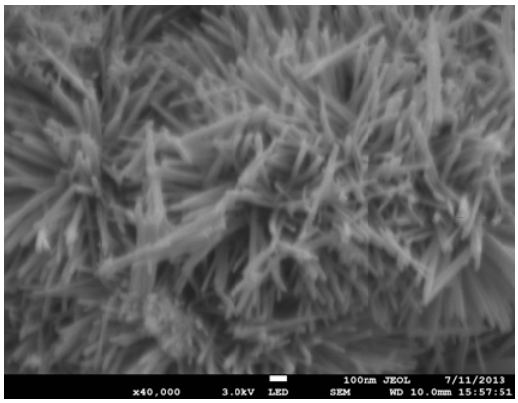

(a)

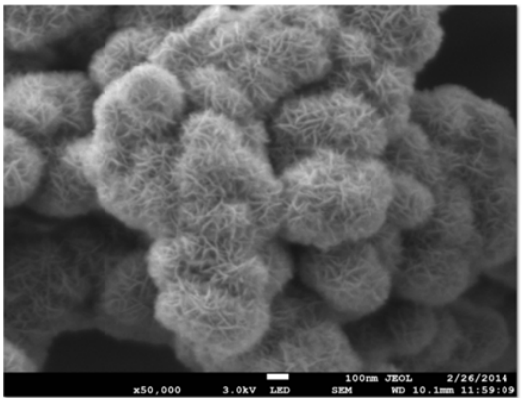

(b)

Fig. 1 FESEM image of: (a) MnO_2 with magnification of 40,000x (urchin-like); (b) Pt/MnO_2 with magnification of 50,000x (cocoon-like)

The MnO_2 nanostructure obtained by hydrothermal method resulted in an urchin-like morphology with many long MnO_2 nanorods radiating from its centre (Fig. 1 (a)). Meanwhile, the surface of urchin-like MnO_2 consisted of a large number of short MnO_2 nanorods that interweave with each other. After Pt doping from sol, the morphology of the catalyst has been changed as shown in Fig. 1 (b). The Pt/MnO_2 nanostructure showed a cocoon-like morphology. The change in morphology might be due to the sol-MnO_2 powder interaction and further processing (washing and drying) of the nanostructure. The change in morphology from urchin-like to cocoon-like might be the advantageous, because the cocoon-like nanostructure possesses higher BET surface area than the urchin-like nanostructure as reported by [15].

B. XRD Analysis of MnO_2 and Pt/MnO_2 Nanostructures

The phase and crystallinity of the as-prepared MnO_2 and Pt-MnO_2 were examined by powder X-ray diffraction and presented in Fig. 2. The sharp diffraction peaks indicate that their crystallinity is high, and the doping process changed the

crystal form. The crystal form of urchin-like MnO_2 can be readily indexed to the pure tetragonal phase of α-MnO_2 (ICDD: 440141), indicating high purity and crystallinity of the final sample. As compared with the XRD patterns of urchin-like MnO_2, the diffraction peaks of 0.8 wt % Pt/MnO2 shift to smaller diffraction angles which might be due to the doping process of Pt onto MnO_2 nanostructure.

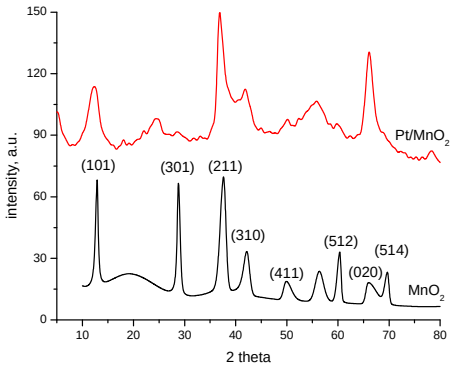

Fig. 2 XRD patterns of MnO_2 and Pt/MnO_2 nanostructures

C.X-Ray Photoelectron Spectroscopy

X-ray photoelectron spectroscopy (XPS) is reported as an effective approach in the investigation of the surface composition and chemical states of solid samples [18]. Besides, information about oxidation state of metal can be obtained through XPS analysis [19]. A typical XPS spectrum of Pt/MnO_2 nanostructured catalyst was measured and the core level spectra of Mn 2p, Pt 4f, and O 1s are depicted in Figs. 3 (a), (b), (c), respectively. Spectra correction was conducted by using internal reference spectra of C 1s at 284.6 eV to compensate the electrostatic charging [20], [21]. The XPS spectra of Mn 2p for Pt-MnO2 as presented in Fig. 3 (a) shows two main peaks centered at 642.5 and 654 eV with a difference in binding energy of 11.5 eV, which could be assigned to Mn $2p_{3/2}$ and Mn $2p_{1/2}$, respectively [22]. The two peaks were in well agreement with those reported in literature, indicating Mn (IV) state for MnO_2 [23]. Fig. 3 (c) presents the deconvoluted XPS O 1s spectra of Pt/MnO_2 centered at 530 eV. The fitting of the spectra gives a sharp peak located at 530 eV and a broad peak at 531.5 eV. The peak at 529-530 eV can be assigned to lattice oxygen while that at 531-532 eV represents to surface oxygen ions or the defect [24]. The deconvoluted XPS spectra of Pt 4f for Pt/MnO_2 was illustrated in Fig. 3 (b) where two peaks of Pt $4f_{7/2}$ and Pt $4f_{5/2}$ were assigned at 71.2 and 74.9 eV, respectively. The findings were consistent with the work done by [25]. The pair of peaks is attributed to Pt (0) or Pt metal nanoparticles which were also reported in [26], [27]. The core level spectra of Pt $4f_{7/2}$ and Pt $4f_{5/2}$ for the bulk Pt are 70.8 and 74.1 eV, respectively [20]. The fitted spectra of Pt $4f_{7/2}$ and Pt $4f_{5/2}$ of current work were shifted to the higher binding energies with respect to those for the bulk Pt. This result indicates an electronic interaction of Pt and the substrates [28].

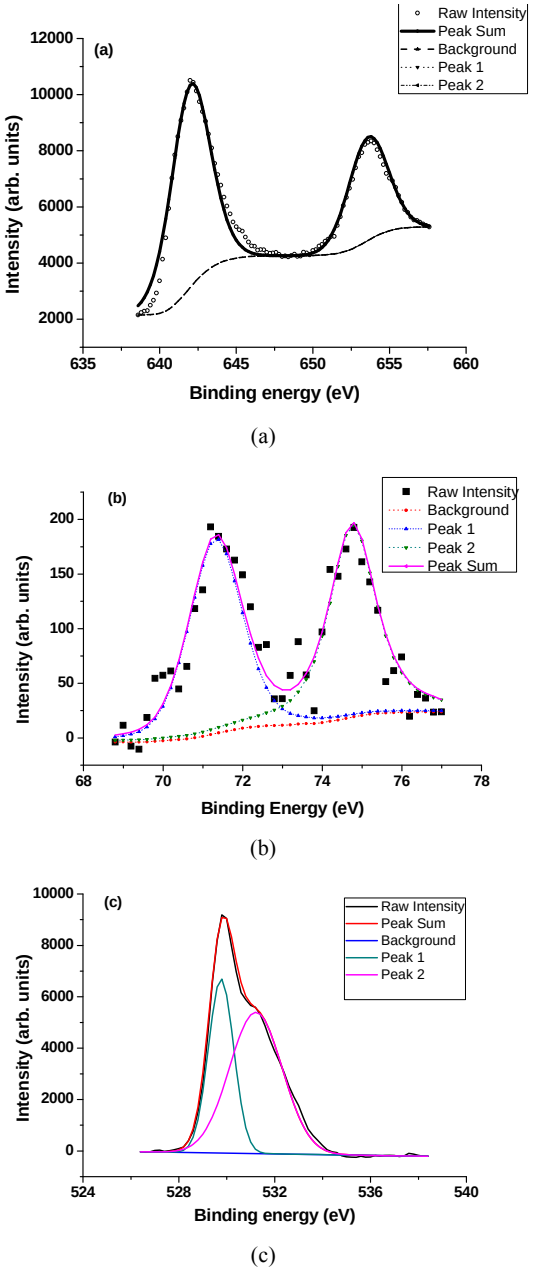

Fig. 3 Deconvoluted XPS spectra of the (a) Mn 2p (b) Pt 4f, and (c) O 1s region

According to [20], the positive shift in binding energy corresponds to a decrease in the electronic charge density on the Pt atoms present in the prepared catalysts. This might arise from metal-support interactions, where there might be an electron shift from the metal to MnO_2 via π-d hybridization.

D.Electrochemical Characterization of the Catalyst by Cyclic Voltammetry

The electrochemical activity of Pt/MnO_2 in the electrolytes was characterized by cyclic voltammogram (CV) approach. The results of the CV of Pt/MnO_2 with different loadings of Pt in 0.1 mol/L Na_2SO_4 saturated by O_2 are shown in Fig. 4 (a).

An obvious oxygen reduction peak of the electrode with MnO_2 and Pt/MnO_2 catalysts is clearly observed at 0.43-0.44 V. The peak is slightly positive for Pt doped catalysts than the MnO_2 catalyst, indicating that the 0.8 wt% Pt/MnO_2 could catalyze ORR at a more positive potential. The current of the ORR at the electrode with 0.4 wt% Pt/MnO_2 catalyst is -0.013 µA, which is two times higher than that of the electrode with MnO_2 catalyst (-0.0056µA). The higher ORR current of the Pt/MnO_2 catalysts could be explained by the specific interaction between Pt with MnO_2 as seen in XPS results (Fig. 3). The CV results with different loadings of Pt in 0.1 mol/L H2SO4 solution saturated by N_2 are shown in Fig. 4 (b). The H+ desorption peak in the range of -0.2 – 0 V is evident for all Pt doped MnO_2 catalysts and the area of the peak was increased with the Pt loading. Table I shows the electrochemical active surface area of Pt/MnO_2 catalysts evaluated in CV where it can be seen that catalyst with higher Pt loading has higher surface area. The high active area of the Pt suggests the formation of Pt nanoparticles on MnO_2 catalyst.

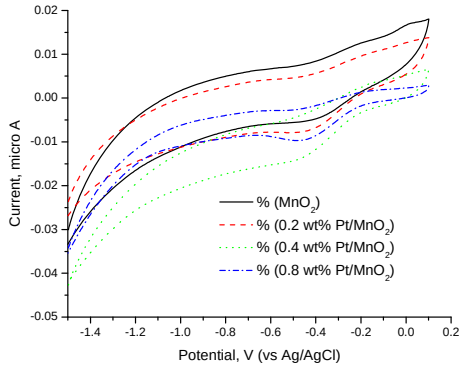

(a)

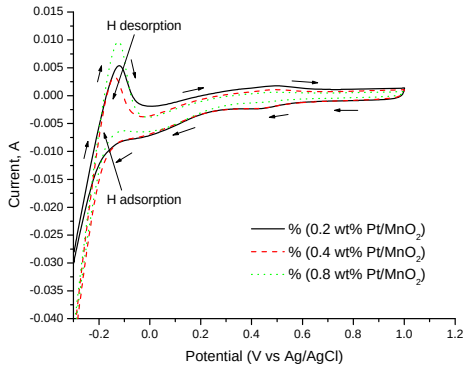

(b)

Fig. 4 Cyclic voltammograms for (a) ORR in 0.1 mol/L Na_2SO_4 saturated by O_2 and (b) in 0.1 mol/L H_2SO_4 solution saturated by N_2 (scan rate = 30 mV/s)

TABLE I
ELECTROCHEMICAL PROPERTIES OF THE CATALYSTS AND THE PERFORMANCE OF AIR-CATHODE MFC

Catalyst	ORR current 10^3, µA	Electrochemical active area, m^2/g	OCV, V	Max.power density, mW/m^3	COD removal eff. , %
MnO_2	-5.6	-	0.402	95	78
0.2 wt% Pt/MnO_2	-7.7	276	0.385	-	79
0.4 wt% Pt/MnO_2	-13.4	550	0.626	165	84
0.8 wt% Pt/MnO_2	-9.7	617	0.602	125	83

E. Performance of Cubic air Cathode Microbial Fuel Cell with Different Cathode Catalysts

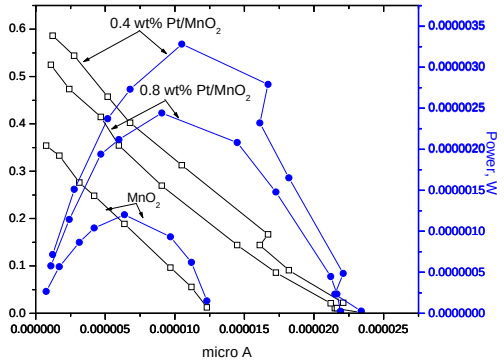

Fig. 5 Polarization and power curves for air-cathode MFCs after 7 days of operation

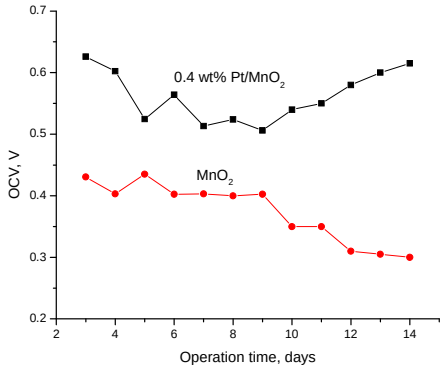

Fig. 6 Open circuit voltage of MFC with Pt/MnO_2 and MnO_2

The MFCs with different cathode catalysts have been operated continuously maintaining same anode condition and cathode catalyst loading. The open circuit voltage and polarization curves were measured regularly. The results are presented in Fig. 5 and Table I. It is clearly evident that the maximum power density and OCV are influenced by the cathode, indicating the limiting role of air-cathode in the MFC under the experimental conditions. The performance order of MFCs with different cathodes is 0.4wt% Pt/MnO_2 > 0.8wt% Pt/MnO_2 > MnO_2 cathode as illustrated in Fig. 5. The results are consistent with the CV results for ORR activity. The OCV of the MFC with 0.4 - 0.8 wt% Pt/MnO_2 cathode was in the range of 0.6 -0.65 V, which was significantly higher compared with MnO_2 cathode. The electrochemical reaction rates could be evaluated by the open circuit voltage (OCV), as [2]

indicated, a higher OCV value is related to a higher reaction rate. Fig. 6 presents the OCV value as a function of time for MFCs with 0.4 wt% Pt/MnO_2 and MnO_2 cathodes. It can be seen that the OCV of the MFC with Pt doped catalyst remained constant even after 14 days of operation, while for the MFC with MnO_2 cathode, dropped significantly within the same duration of operation. The results evidently indicate that the performance of MnO_2 cathode is enhanced due to the Pt doping on MnO_2 as electrocatalyst for ORR. In addition, the COD removal efficiency of 0.4 - 0.8 wt% Pt/MnO_2 -based MFCs was slightly higher than that of MnO_2 -based MFC.

IV. Conclusion

In summary, MnO_2 and Pt/ MnO_2 nanostructured catalysts were successfully synthesized and characterized. The Pt loading and their phases were confirmed by XRD and XPS. XRD revealed the formation of urchin like structure of MnO_2 which transformed to cocoon type phase after Pt doping. The electrochemical active are was increased with the increase in Pt loading. The ORR activity of the 0.4 wt% Pt/MnO_2 catalyst was increased two times compared to MnO_2 catalysts. The catalysts were used in the cathode of the MFC operated with POME as anode substrate. MFC with Pt/MnO_2 (0.4 wt% Pt) as air cathode catalyst generates a maximum power density of 165 mW/ m^3, which is higher than that of MFC with MnO_2 catalyst (95 mW/m^3). The open circuit voltage (OCV) of the MFC operated with MnO_2 cathode gradually decreased during 14 days of operation, whereas the MFC with Pt/MnO_2 cathode remained almost constant throughout the operation suggesting the higher stability of the Pt/MnO_2 catalyst. In view of the outstanding performance of the Pt/MnO_2 catalyst, it has great promising potential in air cathode MFCs without compromising the catalyst cost as aimed.

Acknowledgment

This work was financially supported by research grant from Ministry of Education, Malaysia (Project No: RDU 120611) and Universiti Malaysia Pahang, Malaysia (Project No: RDU 140322).

References

[1] B. E. Logan, Microbial fuel cells, John Wiley & Sons, 2008.
[2] B. E. Logan, B. Hamelers, R. Rozendal, U. Schröder, J. Keller, S. Freguia, P. Aelterman, W. Verstraete, K. Rabaey, "Microbial fuel cells: methodology and technology," *Environmental science & technology*, vol. 40, no. 17, 2006, pp. 5181-5192.
[3] D. Pant, G. Van Bogaert, L. Diels, K. Vanbroekhoven, "A review of the substrates used in microbial fuel cells (MFCs) for sustainable energy production," *Bioresource Technology*, vol. 101, no. 6, 2010, pp. 1533-1543.
[4] S. Oh, B. E. Logan, "Hydrogen and electricity production from a food processing wastewater using fermentation and microbial fuel cell technologies," *Water Research*, vol. 39, no. 19, 2005, pp. 4673-4682.
[5] M. Lu, S. Kharkwal, H. Y. Ng, S. F. Y. Li, "Carbon nanotube supported MnO2 catalysts for oxygen reduction reaction and their applications in microbial fuel cells," *Biosensors and Bioelectronics*, vol. 26, no. 12, 2011, pp. 4728-4732.
[6] X. Wang, Y. Feng, N. Ren, H. Wang, H. Lee, N. Li, Q. Zhao, "Accelerated start-up of two-chambered microbial fuel cells: effect of anodic positive poised potential," *Electrochimica Acta*, vol. 54, no. 3, 2009, pp. 1109-1114.
[7] Q. Wen, Y. Wu, D. Cao, L. Zhao, Q. Sun, "Electricity generation and modeling of microbial fuel cell from continuous beer brewery wastewater," *Bioresource Technology*, vol. 100, no. 18, 2009, pp. 4171-4175.
[8] T. H. Pham, K. Rabaey, P. Aelterman, P. Clauwaert, L. De Schamphelaire, N. Boon, W. Verstraete, "Microbial fuel cells in relation to conventional anaerobic digestion technology," *Engineering in Life Sciences*, vol. 6, no. 3, 2006, pp. 285-292.
[9] D. Pant, A. Adholeya, "Biological approaches for treatment of distillery wastewater: A review," *Bioresource Technology*, vol. 98, no. 12, 2007, pp. 2321-2334.
[10] E. Baranitharan, M. R. Khan, D. M. R. Prasad, J. B. Salihon, "Bioelectricity Generation from Palm Oil Mill Effluent in Microbial Fuel Cell Using Polacrylonitrile Carbon Felt as Electrode," *Water, Air, & Soil Pollution*, vol. 224, no. 5, 2013, pp. 1-11.
[11] R. Bashyam, P. Zelenay, "A class of non-precious metal composite catalysts for fuel cells," *Nature*, vol. 443, no. 7107, 2006, pp. 63-66.
[12] E. HaoYu, S. Cheng, K. Scott, B. Logan, "Microbial fuel cell performance with non-Pt cathode catalysts," *Journal of power sources*, vol. 171, no. 2, 2007, pp. 275-281.
[13] K. Gong, P. Yu, L. Su, S. Xiong, L. Mao, "Polymer-assisted synthesis of manganese dioxide/carbon nanotube nanocomposite with excellent electrocatalytic activity toward reduction of oxygen," *Journal of Physical Chemistry C*, vol. 111, no. 5, 2007, pp. 1882-1887.
[14] F. Cheng, Y. Su, J. Liang, Z. Tao, J. Chen, "MnO2-Based Nanostructures as Catalysts for Electrochemical Oxygen Reduction in Alkaline Media," *Chemistry of Materials*, vol. 22, no. 3, 2009, pp. 898-905.
[15] X. Yu, J. He, D. Wang, Y. Hu, H. Tian, Z. He, "Facile controlled synthesis of Pt/MnO2 nanostructured catalysts and their catalytic performance for oxidative decomposition of formaldehyde," *Journal of Physical Chemistry C*, vol. 116, no. 1, 2011, pp. 851-860.
[16] Y. Chen, C. Liu, F. Li, H.-M. Cheng, "Preparation of single-crystal α-MnO2 nanorods and nanoneedles from aqueous solution," *Journal of Alloys and Compounds*, vol. 397, no. 1, 2005, pp. 282-285.
[17] C.-S. Lin, M. R. Khan, S. D. Lin, "The preparation of Pt nanoparticles by methanol and citrate," *Journal of Colloid and Interface Science*, vol. 299, no. 2, 2006, pp. 678-685.
[18] J. Liqiang, S. Xiaojun, C. Weimin, X. Zili, D. Yaoguo, F. Honggang, "The preparation and characterization of nanoparticle TiO2/Ti films and their photocatalytic activity," *Journal of Physics and Chemistry of Solids*, vol. 64, no. 4, 2003, pp. 615-623.
[19] H. R. Ong, M. R. Khan, M. N. K. Chowdhury, A. Yousuf, C. K. Cheng, "Synthesis and characterization of CuO/C catalyst for the esterification of free fatty acid in rubber seed oil," *Fuel*, vol. 120, no. 2014, pp. 195-201.
[20] Z. Awaludin, M. Suzuki, J. Masud, T. Okajima, T. Ohsaka, "Enhanced electrocatalysis of oxygen reduction on Pt/TaO x/GC," *Journal of Physical Chemistry C*, vol. 115, no. 51, 2011, pp. 25557-25567.
[21] D. A. Pawlak, M. Ito, M. Oku, K. Shimamura, T. Fukuda, "Interpretation of XPS O (1s) in mixed oxides proved on mixed perovskite crystals," *Journal of Physical Chemistry B*, vol. 106, no. 2, 2002, pp. 504-507.
[22] C. Zhou, H. Wang, F. Peng, J. Liang, H. Yu, J. Yang, "MnO2/CNT supported Pt and PtRu nanocatalysts for direct methanol fuel cells," *Langmuir*, vol. 25, no. 13, 2009, pp. 7711-7717.
[23] H. Xia, M. Lai, L. Lu, "Nanoflaky MnO2/carbon nanotube nanocomposites as anode materials for lithium-ion batteries," *Journal of Materials Chemistry*, vol. 20, no. 33, 2010, pp. 6896-6902.
[24] W.-M. Chen, L. Qie, Q.-G. Shao, L.-X. Yuan, W.-X. Zhang, Y.-H. Huang, "Controllable Synthesis of Hollow Bipyramid β-MnO2 and Its High Electrochemical Performance for Lithium Storage," *ACS applied materials & interfaces*, vol. 4, no. 6, 2012, pp. 3047-3053.
[25] P. Bera, K. R. Priolkar, A. Gayen, P. R. Sarode, M. S. Hegde, S. Emura, R. Kumashiro, V. Jayaram, G. N. Subbanna, "Ionic dispersion of Pt over CeO2 by the combustion method: Structural investigation by XRD, TEM, XPS, and EXAFS," *Chemistry of Materials*, vol. 15, no. 10, 2003, pp. 2049-2060.
[26] R. Siburian, J. Nakamura, "Formation Process of Pt Subnano-Clusters on Graphene Nanosheets," *Journal of Physical Chemistry C*, vol. 116, no. 43, 2012, pp. 22947-22953.
[27] R. V. Hull, L. Li, Y. Xing, C. C. Chusuei, "Pt nanoparticle binding on functionalized multiwalled carbon nanotubes," *Chemistry of Materials*, vol. 18, no. 7, 2006, pp. 1780-1788.

[28] E. Antolini, "Formation, microstructural characteristics and stability of carbon supported platinum catalysts for low temperature fuel cells," *Journal of materials science*, vol. 38, no. 14, 2003, pp. 2995-3005.